Toward Parallel Computation of Dense Homotopy Skeletons for nD Digital Objects

Pedro Real[1], Fernando Diaz-del-Rio[2(✉)], and Darian Onchis[3,4]

[1] Institute of Mathematics, University of Seville,
Avda. Reina Mercedes s/n, 41012 Seville, Spain
real@us.es
[2] Computer Architecture and Technology Department,
University of Seville, Avda. Reina Mercedes s/n, 41012 Seville, Spain
fdiaz@us.es
[3] Faculty of Mathematics, Univ. of Vienna,
Oskar-Morgenstern-Platz 1, 1090 Vienna, Austria
[4] Faculty of Mathematics and Computer Science,
West Univ. of Timisoara, Bulevardul Vasile Parvan 4,
300223 Timisoara, Romania

Abstract. An appropriate generalization of the classical notion of abstract cell complex, called primal-dual abstract cell complex (pACC for short) is the combinatorial notion used here for modeling and analyzing the topology of nD digital objects and images. Let $D \subset I$ be a set of n-xels (ROI) and I be a n-dimensional digital image. We design a theoretical parallel algorithm for constructing a topologically meaningful asymmetric pACC $HSF(D)$, called Homological Spanning Forest of D (HSF of D, for short) starting from a canonical symmetric pACC associated to I and based on the application of elementary homotopy operations to activate the pACC processing units. From this HSF-graph representation of D, it is possible to derive complete homology and homotopy information of it. The preprocessing procedure of computing $HSF(I)$ is thoroughly discussed. In this way, a significant advance in understanding how the efficient HSF framework for parallel topological computation of $2D$ digital images developed in [2] can be generalized to higher dimension is made.

Keywords: Computational topology · nD digital image · Primal-dual abstract cell complex · Parallelism · Homological Spanning Forest · Homotopy operation

1 Introduction

The problem of developing a topologically consistent framework for efficient parallel topological analysis and recognition of n-dimensional digital objects is nowadays a major challenge. Intimately associated to this problem, we encounter the issue to find a suitable representation model from which the extraction of

topological features and characteristics of the object can be as fast and the most complete as possible. A successful strategy for achieving these goals is to "cellularize" the images. A primal-dual abstract cell complex [2] (or, pACCs for short), an appropriate generalization of the notion of abstract cell complex [8,9] for describing bitopological spaces, efficiently encodes local topological (incidences between cells, working at sub-n-xel level) information of the digital object in order to be promoted to global consistent topological information. We are mainly interested in information related to "homology holes", which are abstract generalizations at any dimension of the intuitive notion of curve bounding an arc or surface bounding a volume [7]. Classically, the different homology holes of a complex are obtained via linear algebra algorithms based on diagonalization of incidence matrices to Smith Normal Form [17]. The technique employed here for parallel processing is based on building asymmetric pACCs from symmetric ones. The asymmetric and non-redundant output pACCs resulting from our framework encompass the hierarchical graph notion of Homological Spanning Forest (HSF, for short) developed in [10,11,14]. Roughly speaking, an HSF of a digital object is a flexible topological model described by a kind of dense topological skeleton inside the object. Figure 1 shows two different HSFs of the same 2D digital object. The inclusion of an optimal vector field over each tree installed "inside the object" allows us not only counting the different homological holes of dimension 0 (connected components or CCs for short) and dimension 1 but also to removing them via cutting or filling. Moreover, if we retain the vicinity relations between these HSF graphs, we can reach homotopy-based representations of 2D digital images like the adjacency tree of a binary image or the region-adjacency-graph of a grey-level image [13].

In this paper, we design a theoretical parallel algorithm for computing an HSF-structure of a nD-digital object. Let us emphasize that: (a) the HSF-approach can be considered as a Morse-based pre-homology computation method

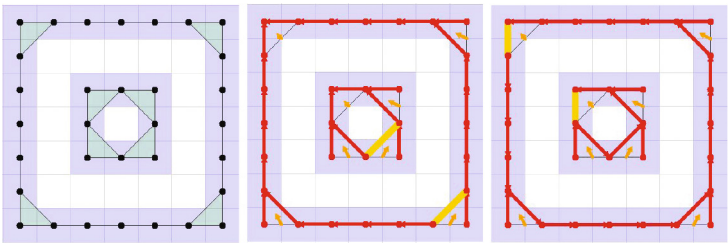

Fig. 1. (Left) ROI consisting in the set of black pixels. The implicit cellularization of the ROI -using 8-adjacency and being the 0-cells the square physical pixels- is superimposed; (Center) Visualization of an HSF of the ROI. The two trees spanning 0-cells (in red) of the ROI mean that it has two 8-CCs. The yellow "trees" -derived from the optimal vector field linking the rest of 1-cells with the set of 2-cells of the ROI- containing a 1-cell marked with a thick yellow segment determine two one-dimensional homological holes of the ROI or, equivalently, two 4-CCs of the background; (Right) Another possible HSF. (Color figure online)

(e.g. [3,4]) in the sense that a discrete vector field is "optimally" installed over the pACC. Its novelty lies in dealing with this issue as a pure combinatorial optimization problem in a fully parallel way over a scenario subdivided space and substituting the classical vector field language of homology by that of the new dynamic notion of crack (called link in [2]); (b) the theoretical time complexity of the parallel algorithm of [2] for computing an HSF structure of a binary digital $n \times m$ image is approximately logarithmic (precisely, $O(log(n+m))$). It seems that its generalization to nD image context can be done without excessive cost in complexity; (c) another strength of this framework is its potentiality to generate new topological representation models of nD objects and images involving homological holes (not only of dimension zero) and topologically strong relationships between them (for instance, generalizing to nD the notions of adjacency tree or RAG 2D models).

A flowchart of this nD-HSF algorithm is shown in Fig. 2.

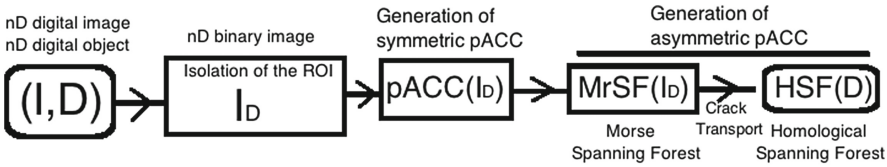

Fig. 2. Workflow of nD-HSF Algorithm.

In what follows, after a section of technical definitions related to the concept of primal-dual abstract cell complex, we formally describe the different stages of the previous theoretical algorithm.

2 Primal-Dual Abstract Cell Complexes

A primal-dual abstract cell complex (pACC, for short) is a suitable generalization of an abstract cell complex and a combinatorial model of a geometric subdivided object as bitopological spaces.

A finite primal-dual abstract cell complex (pACC for short) $\mathsf{C} = (C, {}^{\mathsf{C}}B^p, {}^{\mathsf{C}}B^d, dim_p^{\mathsf{C}}, dim_d^{\mathsf{C}})$ is composed of:

- $C \bigcup \{\emptyset\}$, where C is a finite set of cells and $\emptyset$ is the empty set.
- two dimension functions: *(primal dimension)* $dim_p^{\mathsf{C}} : C \to \{0, 1, 2, \ldots, \ell_p\}$ and *(dual dimension)* $dim_d^{\mathsf{C}} : C \to \{0, 1, 2, \ldots, \ell_d\}$, where $\ell_p, \ell_d \in \mathbb{N} \cup \{0\}$. The set C_i^p (resp. C_i^d) is the set of cells such that their primal (resp. dual) dimension is i.
- two bounding maps: (primal bounding map) a graded function ${}^{\mathsf{C}}B^p = \{{}^{\mathsf{C}}B_i^p\}_i$, such that ${}^{\mathsf{C}}B_i^p : C_i^p \times C_{i+1}^p \to \mathbb{N} \cup \{0\}$ $(\forall 0 \leq i \leq \ell_p - 1)$ and (dual bounding map) a graded function ${}^{\mathsf{C}}B^d = \{{}^{\mathsf{C}}B_i^d\}_i$, such that ${}^{\mathsf{C}}B_i^d : C_i^d \times C_{i+1}^d \to \mathbb{N} \cup \{0\}$, $\forall 0 \leq i \leq \ell_d - 1$. We extend the respective definitions of ${}^{\mathsf{C}}B^p$ and ${}^{\mathsf{C}}B^d$ to

$C \times C$ by simply assigning value zero to the rest of ordered pairs of cells not belonging to the original domains.

The set of values the bounding maps takes on as output is the semi-ring $\mathbb{N} \cup \{0\}$. Of course, it is possible to change the images of the bounding maps to a ring (like $\mathbb{Z}$) or to a field (like $\mathbb{Q}$ o $\mathbb{R}$).

The pACC C is called *uniquely dimensional* if its primal and dual dimensions both depend on *a unique dimension* function $dms : C \to \{0, 1, 2, \ldots, \ell\}$, being $\ell = \ell_p = \ell_d$. ℓ is called *the dimension of* C. In fact, $dim_p = dms$ and $dim_d = \ell - dms$. Let us denote the set of cells C_i^p of primal dimension i simply by C_i and an i-cell means a primal i-cell. A uniquely dimensional pACC C is called *symmetric* if ${}^{\mathsf{C}}B_i^p(c, c') = {}^{\mathsf{C}}B_i^d(c', c)$, $\forall 0 \leq i \leq \ell$ and $\forall c, c' \in C$. In this case, the bounding maps ${}^{\mathsf{C}}B^p$ and ${}^{\mathsf{C}}B^d$ are respectively denoted by ${}^{\mathsf{C}}B$ and ${}^{\mathsf{C}}B^{-1}$.

From now on, to simplify the notation, we drop the subindex i (corresponding to primal dimension) and the superindex C (corresponding to the ACC name) from the dimension and bounding maps, unless otherwise specified.

Given two cells c' and c'' of C, we say that the ordered pair (c', c'') is *an* $(i, i+1)$ *primal (resp. dual) vector* $(i = 0, 1, \ldots)$ of the pACC C if *its primal (resp. dual) multiplicity* $B^p(c', c'') \neq 0$ (resp. if $B^d(c', c'') \neq 0$), being $c' \in C_i^p$ (resp. $c' \in C_i^d$). The cell c' is called the tail and c'' is the head of the primal (resp. dual) vector (c', c''). We say that the set $\{c', c''\}$ is *an* $(i, i+1)$ *primal (resp. dual) incidence set* of the pACC if $B^p(c', c'') \neq 0$ or $B^p(c'', c') \neq 0$ (resp. if $B^d(c', c'') \neq 0$ or $B^d(c'', c') \neq 0$), being c' or c'' a cell of C_i^p (resp. C_i^d).

Given a pACC $\mathsf{C} = (C, B^p, B^d, dim_p, dim_d)$, let us define a sub-pACC $\mathsf{D} = (D, {}^{\mathsf{D}}B^p, {}^{\mathsf{D}}B^d, dim_p, dim_d)$ of C as a new pACC with $D \subset C$ whose: (a) primal and dual dimension functions agree with those of C restricted to D; (b) the primal (resp. dual) bounding map satisfies that if ${}^{\mathsf{D}}B^p(c', c'') = q \neq 0$ (resp. ${}^{\mathsf{D}}B^d(c', c'') = q \neq 0$), then $B^p(c', c'') \geq q$ (resp. $B^d(c', c'') \geq q$). If ${}^{\mathsf{D}}B^p = B^p|_{D \times D}$ and ${}^{\mathsf{D}}B^d = B^d|_{D \times D}$, the sub-pACC D of C is called *complete*.

The complete sub-pACC $St^p(c, \mathsf{C})$ (resp. $St^d(c, \mathsf{C})$) of C, consisting of c and all elements c' in C, such that $B^p(c, c') \neq 0$ (resp. $B^d(c, c') \neq 0$) is called the *primal (resp. dual) open star of* c *in* C. It is exactly the same as the smallest primal (resp. dual) neighborhood of c in C [9]. If C is an uniquely dimensional symmetric pACC, so are $St^p(c, \mathsf{C})$ and $St^d(c, \mathsf{C})$.

Any pACC can be expressed as *a node-arc weighted graph*. The *incidence graph* $G(\mathsf{C})$ associated to a pACC C is the graph such that its nodes are the different cells of C and an edge $\{c, c'\}$ of this graph is either a primal or dual incidence set of the pACC or both. If C is symmetric, we propose as label for an edge $\{c', c''\}$ $(c' \in C_i,\ c'' \in C_{i+1})$ of $G(\mathsf{C})$, the ordered pair $(B^p(c', c''), B^d(c'', c'))$. As weight for a node $c \in C$, we choose the number $dms(c)$.

A *primal (resp. dual) crack* associated to the $(i, i+1)$-primal (resp. dual) vector (c, c') is the set $crk^p(c, c')$ (resp. $crk^d(c, c')$) of triplets (c, c', c''), for all the cells c'' such that (c', c'') is a dual (resp. primal) vector. A crack $crack(c, c')$ can be considered as an uniquely dimensional asymmetric sub-pACC of C. For example, for a primal crack $crk^p(c, c')$, its bounding functions $\bar{B}^p$ and $\bar{B}^d$ satisfy an "ortogonality" condition: for all the triplets (c, c', c'') of $crk^p(c, c')$, $\bar{B}^p(c, c') =$

$B^p(c,c') \neq 0$, $\bar{B}^p(c',c'') = 0$, $\bar{B}^d(c',c'') = B^d(c',c'') \neq 0$, $\bar{B}^d(c,c') = 0$. Let us note that the crack notion is an extension of the term link in [2].

A geometric cell complex $\mathcal{K}$ can be represented by a uniquely dimensional symmetric pACC $\mathsf{K} = (K, B, B^{-1}, dms, \ell - dms)$, such that $B(c',c'') \in \{0,1\}$, $\forall (c',c'') \in K \times K$. In fact, the primal and dual bounding relation maps can automatically be obtained from the complete set of incidences between cells of K which differ in one dimension and the dimension map dms of K agrees with the dimension function of the cell complex $\mathcal{K}$.

Finally, let us note that both bounding graded functions $\{B_i^p\}_i$ and $\{B_j^d\}_j$ of a pACC $\mathsf{C} = (C, B^p, B^d, dim_p, dim_d)$ can be extended to $C \times C$ in an asymmetric, irreflexive and transitive way without difficulty, giving raise to two different (primal and dual) classical ACCs associated to the pACC C. Due to the fact that every finite topological space with the T0-separation property is isomorphic to an abstract cellular complex [9], *a pACC can be interpreted as a finite bitopological space*. The primal and dual ACC of a uniquely dimensional symmetric pACC can be deduced one from each other by simply reversing the order of the factors in the bounding relations.

3 pACC Homotopy Computation

First, we succinctly describe here the distinct steps of the theoretical nD-HSF Algorithm (whose flowchart is (2)). The rest of this section is devoted to understand the concept of elementary homotopy operation and the sequential algorithm computing an HSF of a pACC.

(a) Input data: The pair (I, D). The nD digital image $I : \{1,\ldots,m_1\} \times \{1,\ldots,m_2\} \times \ldots \times \{1,\ldots,m_n\} \rightarrow \{0,1,...,2^c-1\}$ is represented by a $m_1 \times m_2 \times \ldots \times m_n$ $(m_1, m_2, \ldots, m_n, c \in \mathbb{N})$ integer-valued matrix. The digital object D, called region-of-interest (or ROI, for short), is formed by a set of pixels (represented by their corresponding (row,column) coordinates) of I. In fact, in order to avoid the mathematical ill-posed problems of the segmentation and noise, which are ubiquitous in the area of Digital Imagery, I is a pre-segmented digital image, and D is a region of this previous segmentation.

(b) Extraction of the ROI: From I, we "isolate" the ROI D by means of new digital binary image I_D of the same dimension than I. The set of black pixels (numbered by 1's) of I_D is exactly D.

(c) Generation of topological pACCs: In this phase, we compute two kinds of pACCs in this order: (a) first, symmetric pACCs, modeling in a redundant way the connectivity (incidence) information of D and I; (b) finally, asymmetric pACCs, which are non-redundant sub-pACCs of the previous ones, specifying a kind of dense homotopy graph-skeleton of them.

Some key notions for understanding our topological scaffolding are those of primal and dual pACC-homotopy operations. Given a uniquely n-dimensional symmetric pACC $\mathsf{C} = (C, B, B^{-1}, dms, n - dms)$ and a primal vector (c, c'),

then *the primal pACC-homotopy operation* $Op^p(\overrightarrow{(c,c')}(\mathsf{C}))$ is a new symmetric pACC $(C\backslash\{\mathbf{c},\mathbf{c}'\}, \tilde{B}, \tilde{B}^{-1}, dms, n-dms)$, such that the new bounding function $\tilde{B}$ is defined by:

- $\forall \bar{c} \in St^d(\mathbf{c}', \mathsf{C})\backslash\{\mathbf{c}\}$, $\forall \bar{c}' \in St^p(\mathbf{c}, \mathsf{C})\backslash\{\mathbf{c}'\}$,

$$\tilde{B}(\bar{c}, \bar{c}') = B(\bar{c}, \bar{c}') + B(\bar{c}, \mathbf{c}')B^{-1}(\mathbf{c}', \mathbf{c})B(\mathbf{c}, \bar{c}');$$

- for the rest of pairs of cells (c, c'), $\tilde{B}(c, c') = B(c, c')$

Analogously, we can define elementary dual pACC-homotopy operations. We emphasize that such kind of operations is not, in general, a map of pACCs (that is, a map of sets compatible with the dimensions and bounding relations), but it can be considered as a function $Op^p(\overrightarrow{(c,c')}(\mathsf{C})) : pACC \times pACC \to pACC$. For example, considering the primal crack pACC $crk(c, c')$, we can construct a primal pACC-homotopy operation $Op^p(crk(c, c'), \mathsf{C})$ providing us the same resulting pACC than $Op^p(\overrightarrow{(c,c')}(\mathsf{C}))$.

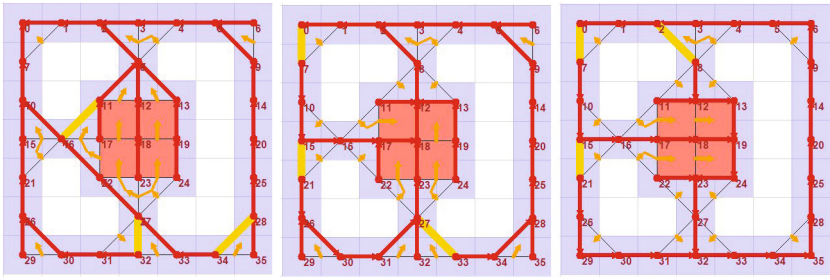

Fig. 3. Three different possible HSF outputs of Algorithm primal-HSF applied to a 2D digital object X of black pixels, depending of the concrete ordered list of cells of X chosen for sequential processing.

Now, we are able to design a sequential computational method for computing an HSF of the pACC $pACC(I_D)$, based on an appropriate reduction of cells via primal homotopy operations.

The output of the previous algorithm consists of a set of asymmetric pACCs $\{\mathcal{F}_{k-1,k}\}_{k=1}^{n}$ and a minimal pACC $\mathcal{H}$ formed by a set of isolated cells of different primal dimension. Figure 3 shows some outputs of the algorithm for 2D objects. The cells of H are called *critical cells*. These data can be reorganized and interpreted in terms of a set $HSF(\mathsf{C})$ of connected sub-graphs spanning the set of cells of C, called *Homological Spanning Forest associated to* C. In fact, these graphs can not be trees in dimension higher than two but we use this name because they appear as a suitable generalization to higher dimension of the notion of the spanning forest as a tool for labeling connected components of a graph [6]. Let us limit ourselves to say that the importance to save this combinatorial homology information of nD digital objects in terms of cracks and graphs primarily lies in

its capacity of creating robust topological models involving homological holes of the objects and strong homology (incidence) relations between them.

For a better understanding, we only work the three-dimensional case in the rest of sections. The nD case is completely analogous.

Algorithm 1. (Sequential pACC-Homology Algorithm)

Input: A uniquely dimensional symmetric pACC $\mathsf{C} := \{C, {}^{\mathsf{C}}B, {}^{\mathsf{C}}B^{-1}, dms, n \backslash dms\}$ *A list of all the cells of* C *ordered by primal dimension* $c_1^0 \dots c_{\ell_0}^0, c_1^1, \dots, c_{\ell_1}^1, \dots c_1^n, \dots, c_{\ell_n}^n$ *such that* $dim_p(c_j^k) = k, \forall k, j$.

1: $\mathsf{H} \leftarrow \mathsf{C}$
2: **for** $k = 1$ to n **do**
3: $\quad \mathcal{F}_{(k-1,k)} \leftarrow \emptyset$
4: $\quad crk \leftarrow \emptyset$
5: $\quad$ **for** $j = 1$ to ℓ_k **do**
6: $\quad\quad$ **if** $\exists \bar{c} \in St^d(c_j^k, \mathsf{H}) / {}^{\mathsf{H}}B(\bar{c}, c_j^k) = 1$ **then**
7: $\quad\quad\quad \mathsf{H} \leftarrow Op^p(crk(\bar{c}, c_j^k), \mathsf{H})$
8: $\quad\quad\quad crk \leftarrow crk \bigoplus \{crk(\bar{c}, c_j^k)\}$;
9: $\quad \mathcal{F}_{(k-1,k)} \leftarrow$ *the incidence graph* $G(crk)$
10: **Output:** $((\mathcal{F}_{(0,1)}, \dots, \mathcal{F}_{(n-1,n)}), \mathcal{H})$

4 Generation of Symmetric pACCs and Parallel Processing Units

The input of the Sequential pACC-Homology Algorithm is a uniquely dimensional symmetric pACC. On the other hand, a fundamental step in the workflow of nD-HSF Algorithm (Fig. 2) is the generation of such objects. Apart from building these initial pACCs, we also create the parallel processing units of our framework.

The scenario in which we need to "embed" the digital image I_D is a uniquely dimensional symmetric pACC intimately associated to the contractible set of cells denoted by $Cell(I_D)$. $Cell(I_D)$ only depends on the dimensions of I_D and can be constructed in a straightforward way. The 0-cells are the voxels (elements of the matrix) of I_D (black or whites), the 1-cells are given by the set of two 6-adjacent voxels (x-frame, y-frame or z-frame adjacent), 2-cells are given by sets of four mutually 6-adjacent voxels and, 3-cells are given by sets of eight mutually 6-adjacent voxels. Thus, a dimension function $dms : Cell(I_D) \rightarrow \{0, 1, 2, 3\}$ is well-defined in this way. In order to create topological coordinates (automatically detecting incidences between cells) preserving the initial coordinate system $(row, colum, depth)$ existing for the voxels of I_D, we use the following geometric realization for the cells of $Cell(I_D)$: (a) 0-cells are points in $\mathbb{R}^3$ with natural-value coordinates; (b) a 1-cell is represented at sub-voxel level by the coordinates of the barycenter of the segment determined by its corresponding pair of voxels, (c) a 2-cell is represented at sub-voxel level by the coordinates of

the barycenter of the square formed by the 4-uple of voxels barycenters; (d) a 3-cell is represented at sub-voxel level by the coordinates of the barycenter of the cube formed by its corresponding 8-uple of voxels. For instance, a 1-cell is specified by topological coordinates of the type (x_1, x_2, x_3), where two value of them are natural numbers and the third is a natural number minus $\frac{1}{2}$ (for example, x_3). The geometric boundary of this 1-cell which is formed by the set of two 0-cells $\{(x_1, x_2, x_3 - \frac{1}{2}), (x_1, x_2, x_3 + \frac{1}{2})\}$ completely describes the dual bounding relation of the 1-cell. Its geometric coboundary, formed by the set of four 2-cells $\{(x_1 \pm \frac{1}{2}, x_2, x_3), (x_1, x_2 \pm \frac{1}{2}, x_3 + \frac{1}{2})\}$ fully specifies its primal bounding relation. Then, it is straightforward to construct the uniquely dimensional symmetric pACC $pACC(I_D) = (Cell(I_D), B_{I_D}, B_{I_D}^{-1}, dim_p^{I_D}, dim_d^{I_D})$. Notice that $pACC(I_D) = pACC(I)$, and, in consequence, $pACC(I_D)$ is independent of D. We can also define another uniquely dimensional symmetric sub-pACC $pACC(D)$ of $pACC(I_D)$, being $Cell(D)$ its set of cells. $Cell(D)$ is the *topological hull of the set of black voxels* D within I_D, which means that the 0-cells of $Cell(D)$ are the black voxels of I_D and its i-cells c $(i = 1, 2, 3)$ can be recursively defined in terms of $(i-1)$-cells by imposing that $St^d(c) \subset Cell(D)$.

Any node (i-cell) (x, y, z) of the incidence graph $G(pACC(I_D))$ has the number $color(x, y, z)$ as weight. The function $color : Cell(I_D) \to \{0, \frac{1}{2}, 1\}$ is defined as follows: (a) for a 0-cell, it is the voxel value in I_D; (b) for an i-cell c with $i \geq 1$, if all the values of the color function over the 0-cells of c is 0 (resp. 1), then $color(c)$ is 0 (resp. is 1). In another case, $color(c) = \frac{1}{2}$.

For creating the parallel processing units, the idea is to establish a regular partition of the $Cell(I_D)$ into *cellular units* $Cell(x, y, z)$. There are as many cellular units as voxels the image has (equivalently, as 0-cells the $pACC(I_D)$ has). The *cellular unit* $Cell_8(x, y, z)$ associated to the voxel of topological coordinates (x, y, z) is the set $\{(x, y, z), (x+\frac{1}{2}, y, z), (x, y+\frac{1}{2}, z), (x, y, z+\frac{1}{2}), (x+\frac{1}{2}, y+\frac{1}{2}, z), (x+\frac{1}{2}, y, z+\frac{1}{2}), (x, y+\frac{1}{2}, z+\frac{1}{2}), (x+\frac{1}{2}, y+\frac{1}{2}, z+\frac{1}{2})\}$ (one 0-cell, three 1-cells, three 2-cells, one 3-cell). Considered as an uniquely dimensional asymmetric sub-pACC of $pACC(I_D)$, *the processing unit* $\mathsf{PE}(x, y, z)$ is defined as the sum of pACCs $\bigoplus_{(c', c'') \in U} crk^p(c', c'')$, where $U = Cell_8(x, y, z) \times Cell_8(x, y, z)$. Its underlying set of cells involves 27 cells which belong to the topological hull generated by the cells (x, y, z), $(x+1, y, z)$, $(x, y+1, z)$, $(x, y, z+1)$, $(x+1, y+1, z)$, $(x+1, y, z+1)$, $(x, y+1, z+1)$ and $(x+1, y+1, z+1)$. The number of primal vectors (see Fig. 4) involved in $\mathsf{PE}(x, y, z)$ is twelve (three $(0, 1)$ vectors, six $(1, 2)$ vectors and three $(2, 3)$ vectors).

5 Generation of MrSFs

The next step in the Algorithm nD-HSF is the parallel building of an HSF of the initial geometric symmetric pACC $pACC(I_D)$. This particular asymmetric pACC $MrSF(I_D)$ is called Morse Spanning Forest (MrSF for short). An MrSF has the property that the set of its elementary primal cracks applied in some order in a sequential process of reduction based on primal homotopy operations provides a final pACC consisting in only one 0-cell (critical cell). In this way,

a MrSF for I_D is seen as a kind of "dense combinatorial skeleton" of the contractible cell complex $Cell(I_D)$. This notion has been already developed in [12] making use exclusively of homological arguments. Finally, the last process of the pipeline of Fig. 2, called *crack transport*, consists in a "homotopy optimization" of $MrSF(I_D)$ in order to get another MrSF, denoted by $HSF(I_D)$, such that its restriction to $Cell(D)$ is a true HSF $HSF(D)$ of D. This optimization is done by suitably "transporting" cracks of the $MrSF(I_D)$, with the objective to maximize the number of its primal bounding relations between cells of $pACC(D)$. We focus here in the parallel algorithmic techniques for MrSF construction; the crack transport step of the algorithm will be studied in detail elsewhere.

A *Morse Spanning Forest* for a three dimensional digital image I of dimension $m_1 \times m_2 \times m_3$ is any output $((\mathcal{F}_{(0,1)}, \mathcal{F}_{(1,2)}, \mathcal{F}_{(2,3)}), \mathcal{H})$ of Sequential pACC-Homology Algorithm applied to $pACC(I)$. It is not difficult to prove that any MrSF has only one $(0,1)$-tree.

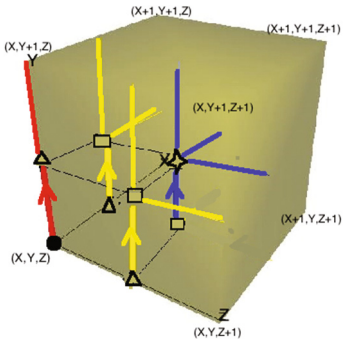

Fig. 4. An activation state (local MrSF rule: direction +Y) of the processing unit $PE(x, y, z)$ showing its eight active cells, primal and dual activation vectors and associated cracks. The 0-cell (x, y, z) is drawn with a circle, the 1-cells with triangles, the 2-cells with squares and the 3-cell with a star. The active primal vectors are drawn with an arrow and using different colors depending on its dimension.

Our algorithm of MrSF generation is divided into two main steps: (a) building a MrSF at local (voxel's neighborhood) level by means of a process of activation of processing units; (b) building the MrSF at global level, specifying the membership of any cell to the corresponding tree of the MrSF. Afterwards, we can proceed to the Final HSF determination via crack transports.

(a) MrSF building at local level: Activation of processing units. There are nine possible activation states for any $\mathsf{PE}(x, y, z)$, each one associated to a particular configuration of four disjoint primal vectors (called primal activation vectors) involving cells of $Cell_8(x, y, z)$. The sum of the crack pACCs of $\mathsf{PE}(x, y, z)$ associated to these primal activation vectors fully defines the corresponding activation state.

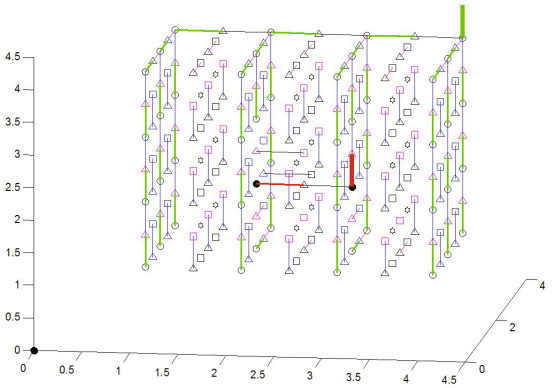

Fig. 5. A (4,3,4) binary 3D image showing active primal $(0,1)$-vectors (red and green colors) and dual $(1,0)$-vectors (black thin vectors) of the MrSF. Thicker vectors indicate possible critical 0-cells. (Color figure online)

For activating in parallel all the processing units of $pACC(I_D)$, we can use *local MrSF rules*. For each $\mathsf{PE}(x,y,z)$, we choose an activation's state depending of giving preference to some order in the principal directions or the particular configuration of the color function of the cells in $\mathsf{PE}(x,y,z)$ (Fig. 4).

In our current implementation of the algorithm of MrSF generation: (a) the local MrSF rules are first defined for the lowest dimension cells and then progressively extended to higher dimension; (b) we give preference to $+Z$ direction, then to $+Y$, and finally to $+X$.

Once the primal $(0,1)$-vector of the $\mathsf{PE}(x,y,z)$ is activated, the two primal $(1,2)$-vectors and the $(2,3)$-vector are activated following the same direction of the first one. This implies that only one 1-cell of $Cell_8(x,y,z)$ belong to the $(0,1)$-tree of the MrSF, and the other two 1-cells reside in the $(1,2)$-tree. Figure 5 shows an example of the primal $(0,1)$ and $(1,2)$ vectors for a binary 3D image that contains two black voxels in the center.

The above MrSF arrangement is one the many possible configurations. Its main advantage is that it can be computed in a fully parallel manner for each voxel. Other possibilities can be exploited, but the parallelism feature should be preserved if we would want to process real 3D images in an efficient way.

(b) Global MrSF construction. Once a local MrSF has been defined it is necessary to introduce global relations between the cells of the whole MrSF. This process can be done in a similar way to that of [2]. That algorithm was much easier since it was written only for two dimensional images. Nevertheless, the idea is the same: to label each cell of the incidence graph (forest) $G(MrSF)$ of the MrSF, according to its membership to some connected subgraph (tree) of $G(MrSF)$. At the end of this process, the different connected components of $G(MrSF)$ must have been labeled (Fig. 6).

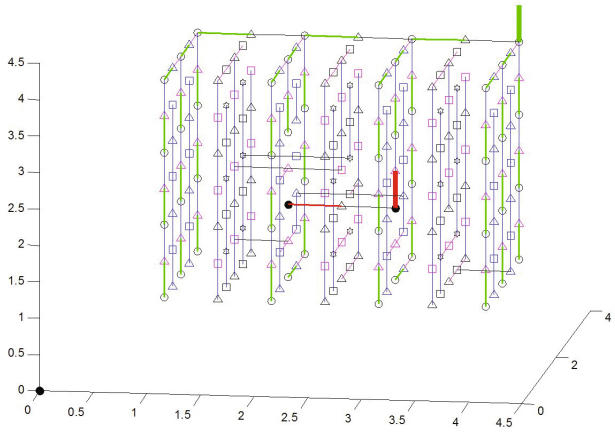

Fig. 6. The same (4,3,4) binary 3D image of Fig. 5 with the complete MrSF. Thicker links indicate potential critical 0-cells.

(c) Final HSF determination via crack transports. This final step of the nD-HSF Algorithm is aimed to minimize the number of critical cells. This would produce the final HSF. As an example, the trees of Fig. 7(Left) would transform into that of Fig. 7(Right). A graphical explanation of this process from the lower dimensional MrSF trees to the higher ones is the following. Firstly, the $(0,1)$-crack marked as 'D' is transported to the right inferior crack in the $(0,1)$-tree. Secondly, the crack 'C' is laid to its left to continue the closing of the 0–1 tree. Transports of 'C' and 'D' supposes the cancellation of one critical 0-cell and one critical 1-cell. In fact, these cells should be detected as false critical cells in the initial MrSF. This transport process is really a pairing of critical cells of different dimensions going through the corresponding tree. Finally, cracks 'A' and 'B' must be also transported so as to "close" properly the 1–2 tree. This yields to an equivalent set of trees, which composed the HSF for the ROI. Obviously this final HSF indicates that the ROI contains only one critical 0-cell being the

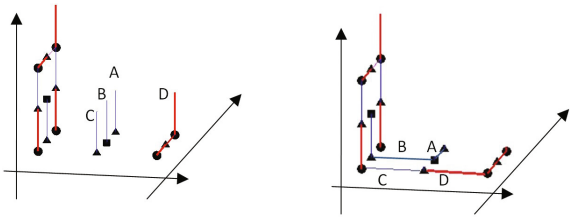

Fig. 7. (Left) A ROI (composed of 6 voxels in 'L' shape) that contains only one CC, and whose MrSF presents two separated 0–1 trees. Cracks that go out from the ROI indicate possible critical cells. (Right) The same 3D image that contains only one 0–1 tree after the necessary transports that complete the HSF.

representative of the CC (connected component). The correct computation of final HSF will yield to the homology of any CC inside a digital image. Some examples are shown in the next section.

6 Examples of Homological Magnitudes of Several Shapes Obtained Through 3-Dimensional HSFs

The topological nature of 3D digital images are much richer than that of 2-D images. Attending exclusively to homology groups, apart from cavities and connected components of a digital object (somewhat comparable to holes and connected components in 2D imagery context), tunnels appear in 3D. In a nutshell, each critical cell of any dimension is in direct relationship with a different homology generator. Figure 8 and 9 shows different shapes and their corresponding critical cells (those belonging to a crack of a MrSF "going out" of the ROI). To ease the viewing of these figures, only ROIs are represented and axes are not drawn. Cells belonging to the black ROI have been filled. These results are summarized in Table 1. Table 1 shows the results of the different simple shapes of Figs. 8 to 9 and their critical cells. Excepting Fig. 9 Left (due to its false critical cells), the number of critical 0-cells agree with the number of CCs, the number of

Table 1. Results of the different simple shapes of Figs. 8 and 9 and their critical cells

Shapes	# Critical 0-cells	# Critical 1-cells	# Critical 2-cells
Two perpendicular rings with contact	1	2	0
Two perpendicular crossing rings	2	2	0
An empty polyhedron (showing its MrSF)	1	2	3
An emptypolyhedron (showing its HSF)	1	2	0

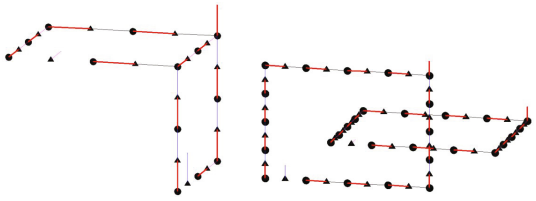

Fig. 8. Left: Two perpendicular 3×3 rings with contact resulting in two critical 1-cells (inferior right corner and superior left corner), representative of its two tunnels, and one critical 0-cell (upper right corner), representative of the CC. Right: Two perpendicular crossing 3×3 rings resulting in two critical 1-cells (inferior left corners), representative of two tunnels, and two critical 0-cells (upper right corners), representative of the two CCs.

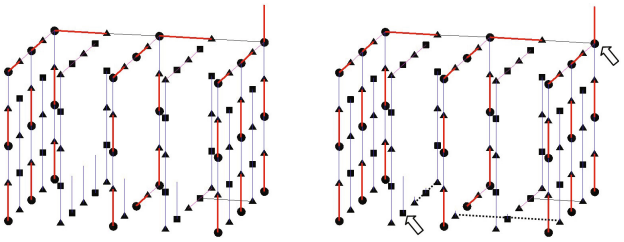

Fig. 9. Left: A MrSF of an empty $3 \times 3 \times 3$ polyhedron. There is one critical 0-cell (upper right corner), representative of the CC. In addition, three critical 2-cells and two 3 critical 1-cells (all of them in the inferior side) have appeared. Two pairs of them are false critical cells. Right: After proper transports (marked with thicker dotted lines), the HSF of the same empty polyhedron yields to only one critical 2-cell (representative of the cavity), and the same critical 0-cell. Arrows indicates the position of these resultant critical cells.

critical 1-cells indicates the number of tunnels and the number of critical 2-cells represents the number of cavities.

7 Conclusions

Based on the notions of primal-dual abstract cell complex and homotopy operation, and generalizing to higher dimension the work developed in [2], a theoretical algorithm for computing combinatorial homology structures, called HSFs of nD digital objects, has been sketched. Focusing in a topological pre-processing step, called Morse Spanning Forest generation, we set a fully parallel algorithm for determining a kind of dense topological skeleton associated to the image scenario within which the digital object is embedded. Both to analyze the efficiency of the procedure and to advance in increasing the degree of understanding on HSF or pACC homology computation of digital objects, an unpretentious implementation done in Matlab is used for experimentation. Although a theoretical complexity study of the parallel algorithm has not yet been carried out, the encouraging results obtained in [2] allow us to be optimistic in computing the HSF information in a fast way. Concerning the computation of algebraic homology holes with coefficients in a ring or a field and that of "homotopy holes" of objects (those related to generalized "parametrized and oriented closed curves" [7]), they sound theoretically attainable from HSF-graph information. An argument supporting this idea is the fact that an HSF structure can be algebraically interpreted (allowing formal sums of cells with coefficients in some ground ring or field) as an operator controlling a chain homotopy equivalence between an object and its homology [1,5,12,15,16]. Finally, the possibility to detect homological hole relationships (like adjacency or "to be surrounded by" between path connected components in 2D) in an HSF allows holding high expectations in achieving functional implementations of parallel algorithms of topological pattern recognition based on HSF information.

Acknowledgments. This work has been supported by the Spanish research projects (supported by the Ministerio de Economía y Competitividad and FEDER funds) COFNET (Event-based Cognitive Visual and Auditory Sensory Fusion, TEC2016-77785-P) and TOP4COG (Topological Recognition of 4D Digital Images via HSF model, MTM2016-81030-P (AEI/FEDER,UE)). The last co-author gratefully acknowledges the support of the Austrian Science Fund FWF-P27516.

References

1. Berciano, A., Molina-Abril, H., Real, P.: Searching high order invariants in computer imagery. Appl. Algebra Eng. Commun. Comput. **23**(1–2), 17–28 (2012)
2. Díaz-del-Río, F., Real, P., Onchis, D.: A parallel homological spanning forest framework for 2D topological image analysis. Pattern Recogn. Lett. **83**, 49–58 (2016)
3. Harker, S., Mischaikow, K., Mrozek, M., Nanda, V., Wagner, H., Juda, M., Dlotko, P.: The efficiency of a homology algorithm based on discrete Morse theory and coreductions. Image-A: Appl. Math. Image Eng. **1**(1), 41–48 (2010)
4. Floriani, L., Fugacci, U., Iuricich, F.: Homological shape analysis through discrete morse theory. In: Breuß, M., Bruckstein, A., Maragos, P., Wuhrer, S. (eds.) Perspectives in Shape Analysis. MV, pp. 187–209. Springer, Cham (2016). doi:10.1007/978-3-319-24726-7_9
5. González-Díaz, R., Real, P.: On the cohomology of 3D digital images. Discrete Appl. Math. **147**(2), 245–263 (2005)
6. Hopcroft, J., Tarjan, R.: Algorithm 447: efficient algorithms for graph manipulation. Commun. ACM **16**(6), 372–378 (1973)
7. Hurewicz, W.: Homology and homotopy theory. In Proceedings of the International Mathematical Congress of 1950, p. 344. University of Toronto Press (1952)
8. Klette, R.: Cell complexes through time. In International Symposium on Optical Science and Technology. International Society for Optics and Photonics, pp. 134–145 (2000)
9. Kovalevsky, V.: Finite topology as applied to image analysis. Comput. Vis. Graph. Image Process. **46**, 141–161 (1989)
10. Molina-Abril, H., Real, P., Nakamura, A., Klette, R.: Connectivity calculus of fractal polyhedrons. Pattern Recogn. **48**(4), 1150–1160 (2015)
11. Molina-Abril, H., Real, P.: Homological spanning forest framework for 2D image analysis. Ann. Math. Artif. Intell. **64**(4), 385–409 (2012)
12. Molina-Abril, H., Real, P.: Homological optimality in Discrete Morse Theory through chain homotopies. Pattern Recogn. Lett. **11**, 1501–1506 (2012)
13. Pavlidis, T.: Algorithms for Graphics and Image Processing. Springer Science and Business Media, Heidelberg (1977)
14. Real, P., Molina-Abril, H., Gonzalez-Lorenzo, A., Bac, A., Mari, J.L.: Searching combinatorial optimality using graph-based homology information. Appl. Algebra Eng. Comm. Comp. **26**(1–2), 103–120 (2015)
15. Real, P.: Homological perturbation theory and associativity. Homology, Homotopy Appl. **2**(1), 51–88 (2000)
16. Real, P.: An algorithm computing homotopy groups. Math. Comput. Simul. **42**(4–6), 461–465 (1996)
17. Veblen, O.: Analisis Situs, vol. 5. A.M.S. Publications, Providence (1931)